nature publishing group

Copper-trafficking efficacy of copper-pyruvaldehyde bis(N^4-methylthiosemicarbazone) on the macular mouse, an animal model of Menkes disease

Mitsutoshi Munakata[1], Hiroko Kodama[2], Chie Fujisawa[2], Tomoko Hiroki[2], Kazuhiko Kimura[3], Mika Watanabe[4], Masazumi Nishikawa[5] and Shigeru Tsuchiya[1]

BACKGROUND: Menkes disease (MD) is a disorder of copper transport caused by ATP7A mutations. Although parenteral copper supplements are partly effective in treating MD, the copper level in the brain remains insufficient, whereas copper accumulates in the kidney. We investigated the copper-trafficking efficacy of copper-pyruvaldehyde bis(N^4-methylthiosemicarbazone) (Cu-PTSM), a lipophilic copper complex, in macular mice, an animal model of MD.

METHODS: Macular mice were treated with cupric chloride ($CuCl_2$) or Cu-PTSM on postnatal days 4, 10, and 17. At 4 wk of age, the copper levels in major organs and cytochrome oxidase (CO) activity in brain tissue were measured. Hematology, blood biochemistry, and urinary β2-microglobulin (β2-M) secretion were also assessed.

RESULTS: The copper levels in the brains of the Cu-PTSM-treated group remained low, but CO activity in the cerebral and cerebellar cortices in the Cu-PTSM-treated group were higher than those in the $CuCl_2$-treated group. There were no significant differences in hematological or biochemical findings or in urinary β2-M secretion among the groups.

CONCLUSION: Although the copper-trafficking efficacy of Cu-PTSM was limited, the improved CO activity in the brain suggests that Cu-PTSM delivered copper more effectively to neuronal CO than did $CuCl_2$. Reduced renal copper accumulation may be beneficial in prolonged copper supplementation.

Menkes disease (MD) is an X-linked recessive disorder of copper transport caused by mutations in a gene encoding copper-transporting P-type ATPase (ATP7A). ATP7A is expressed in most cell types, although not in hepatocytes (1), and is located primarily in the *trans*-Golgi network, where it transports copper in from the cytosol (2). Under conditions in which copper levels are elevated, ATP7A relocalizes to the plasma membrane to expel copper from the cell. Therefore, ATP7A dysfunction causes severe problems in multiple aspects of copper trafficking, such as intestinal absorption, renal excretion, and passage through the blood–brain barrier (3).

Attempts at therapy for MD have focused on copper replacement. Subcutaneous injection of copper-histidine ameliorates the natural history of MD when started in early infancy (4,5). However, penetration of copper into the brain remains insufficient due to impaired copper transport after the blood–brain barrier becomes mature, whereas copper abnormally accumulates in the kidneys and the intestine (6). To overcome the insufficient copper distribution to the brain, diethyldithiocarbamate, a lipid-soluble chelator, has been proposed in combination with copper replacement therapy. This compound significantly increases copper levels in the brain, although the copper accumulation in the kidney remains high (6,7).

Copper-pyruvaldehyde bis(N^4-methylthiosemicarbazone) (Cu-PTSM; **Figure 1**) labeled with copper radioisotopes is a radiopharmaceutical used in positron emission tomography imaging of the brain and heart (8,9). Cu-PTSM is an organic complex that is neutral and highly lipophilic, so it readily passes through the cell membrane. When Cu-PTSM reaches the cell, it is irreversibly reduced and cleaved to liberate copper, which is incorporated into intracellular copper pools (10,11). These unique characteristics of Cu-PTSM suggested that non-radiolabeled Cu-PTSM could be used as a carrier for copper.

A wide variety of animal models for MD have been developed (1,12). Among them, macular mice are one of the closest models to the classical form of MD; hemizygous males exhibit MD-related symptoms and require copper injections early in life to survive (13–15). In this study, we investigated the copper-trafficking efficacy of Cu-PTSM to the critical organs in macular mice.

RESULTS

Acute Toxicity Studies in Normal C3H Mice

Saline, dimethyl sulfoxide (DMSO), cupric chloride ($CuCl_2$), or Cu-PTSM was injected subcutaneously into normal male C3H mice (15–17 d old, n = 14–16 in each group) at the same doses as used in macular mouse treatment in this study. In blood sampled at 24 h after injection, there was no significant

[1]Department of Pediatrics, Tohoku University School of Medicine, Sendai, Japan; [2]Department of Pediatrics, Teikyo University School of Medicine, Tokyo, Japan; [3]Department of Farm Management, School of Food, Agricultural and Environmental Sciences, Miyagi University, Sendai, Japan; [4]Department of Pathology, Tohoku University School of Medicine, Sendai, Japan; [5]Depertment of Food Management, School of Food, Agricultural and Environmental Sciences, Miyagi University, Sendai, Japan. Correspondence: Mitsutoshi Munakata (m-munakata@umin.ac.jp)

Received 4 April 2012; accepted 4 May 2012; advance online publication 25 July 2012. doi:10.1038/pr.2012.85

difference in laboratory values among the groups at the doses used (Table 1).

Body and Organ Weights of $CuCl_2$- and Cu-PTSM-Treated Macular Mice

The bodies and organs of $CuCl_2$- and Cu-PTSM-treated macular mice were weighed and compared with normal male littermate mice at 4 wk of age (n = 8 in each group). In the control group, body weight reached 20.6 ± 2.0 g vs. 10.4 ± 2.5 and 13.3 ± 3.3 g in the $CuCl_2$- and Cu-PTSM-treated groups, respectively. The body weights in the $CuCl_2$-treated and Cu-PTSM-treated groups were significantly lower than the controls, whereas there was no significant difference between the $CuCl_2$- and Cu-PTSM-treated groups. Figure 2 shows the organ weights of the control, $CuCl_2$-, and Cu-PTSM-treated mice at 4 wk of age. The cerebrum weights of the $CuCl_2$- and Cu-PTSM-treated groups were significantly lower than those of the controls, whereas the cerebellum weights did not differ among the groups. The kidney weights of the $CuCl_2$- and Cu-PTSM-treated groups were slightly lower than those of the controls.

Organ Copper Concentrations in $CuCl_2$- and Cu-PTSM-Treated Macular Mice

Figure 3 summarizes the copper concentrations in the major organs (n = 8). Copper levels in the cerebrum and cerebellum were significantly lower in both $CuCl_2$- and Cu-PTSM-treated groups than in controls. No significant difference in copper levels was found between the cerebrum or cerebellum of $CuCl_2$-treated and those of Cu-PTSM-treated groups. Conversely, the copper levels in the kidneys of $CuCl_2$- and Cu-PTSM-treated groups were significantly higher than in those of the controls, but the copper level in the Cu-PTSM-treated group was nearly half that of the $CuCl_2$-treated group ($P < 0.001$).

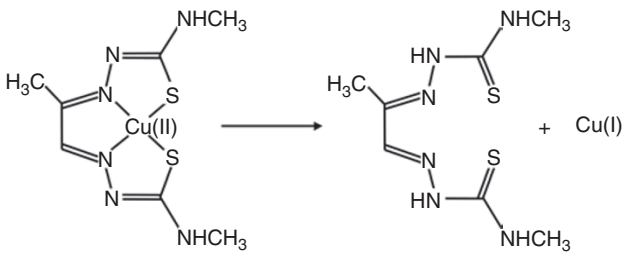

Figure 1. Chemical structures of copper-pyruvaldehyde bis(N^4-methylthiosemicarbazone) complex (Cu-PTSM). Cu-PTSM is a stable, neutral lipophilic compound (left) and therefore diffuses through the cell membrane. When Cu-PTSM is reduced within cells, it becomes labile and releases copper (right).

Effect of Cu-PTSM on Cytochrome Oxidase Activity in the Cerebral and Cerebellar Cortex

Figure 4a,b shows the histological appearance of the cerebral cortex and the cerebellar hemispheric cortex stained for cytochrome oxidase (CO) histochemistry. In the control mice, layer IV of the cerebral cortex showed the densest staining among the layers. The macular mice treated with $CuCl_2$- or Cu-PTSM showed less intense staining than the controls. However, the tissue staining in the Cu-PTSM-treated group was denser than that in the $CuCl_2$-treated group. Similarly, the molecular layer of the cerebellar cortex in the Cu-PTSM-treated group showed stronger staining than that of the $CuCl_2$-treated group. No obvious difference in the tissue staining was observed among the granular layers of the three experimental groups.

Figure 4c–e summarizes the results of CO activity measurements (n = 8). Optical density was measured in layer IV of the cortex. Although the levels of CO activity in both the $CuCl_2$- and Cu-PTSM-treated groups were lower than that in the control group, the activity in the Cu-PTSM-treated group was significantly higher than that in the $CuCl_2$-treated group. Similarly, CO activity in the cerebellar cortex molecular layer of the Cu-PTSM-treated group was significantly higher than that in the $CuCl_2$-treated group. No significant difference was found in the granular layers among the three experimental groups.

Effects of $CuCl_2$ or Cu-PTSM Treatment on Major Organs in Macular Mice

Table 2 shows laboratory values at 4 wk in mice treated with $CuCl_2$ or Cu-PTSM. No significant differences were detected

Table 1. Acute effects of $CuCl_2$, Cu-PTSM, and solvents on hematological and biochemistry data in normal C3H mice

	Controls	DMSO	$CuCl_2$	Cu-PTSM	P value
WBC (10^3/mm^3)	2.9 ± 0.8	3.1 ± 0.8	2.9 ± 0.7	3.0 ± 0.7	0.99
RBC (10^6/mm^3)	5.9 ± 0.5	6.0 ± 0.6	6.0 ± 0.8	6.1 ± 0.8	0.95
Hb (g/dl)	11.3 ± 1.2	11.6 ± 1.0	11.2 ± 1.6	11.5 ± 1.6	0.97
Hct (%)	32.2 ± 4.0	33.3 ± 4.3	33.1 ± 6.1	33.5 ± 6.0	0.99
Plt (10^3/mm^3)	472 ± 150	485 ± 102	524 ± 118	472 ± 92	0.85
AST (IU/l)	70.9 ± 11.4	69.5 ± 18.3	69.8 ± 14.0	63.4 ± 10.6	0.62
ALT (IU/l)	30.3 ± 12.1	32.0 ± 18.8	35.5 ± 16.3	36.2 ± 11.5	0.54
BUN (mg/dl)	22.9 ± 5.6	21.4 ± 5.0	20.5 ± 5.9	20.9 ± 5.4	0.28
Cr (mg/dl)	0.15 ± 0.03	016 ± 0.04	0.15 ± 0.03	0.15 ± 0.04	0.92

Data are shown as mean ± SD (n = 14–16). P values were determined using the Kruskal–Wallis test.

ALT, alanine aminotransferase; AST, aspartate aminotransferase; BUN, blood urea nitrogen; Cr, creatinine; $CuCl_2$, cupric chloride; Cu-PTSM, copper-pyruvaldehyde bis(N^4-methylthiosemicarbazone); DMSO, dimethyl sulfoxide; Hb, hemoglobin concentration; Hct, hematocrit; Plt, platelets; RBC, red blood cell counts; WBC, white blood cell counts.

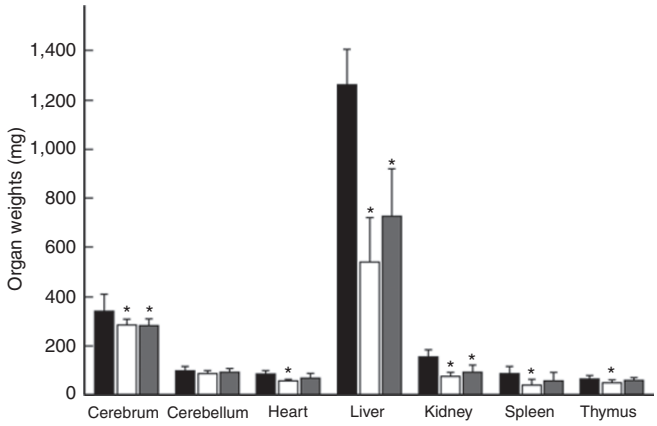

Figure 2. Organ weights of control male mice and macular mice treated with cupric chloride ($CuCl_2$) or copper-pyruvaldehyde bis(N^4-methylthiosemicarbazone) (Cu-PTSM). Weights of the control (black bar), $CuCl_2$-treated (white bar), and Cu-PTSM-treated mice (gray bar) are shown as means ± SD (in mg, $n = 8$). *$P < 0.05$, $CuCl_2$-treated or Cu-PTSM-treated groups vs. control group. No significant difference was detected between $CuCl_2$-treated and Cu-PTSM-treated groups in any organ.

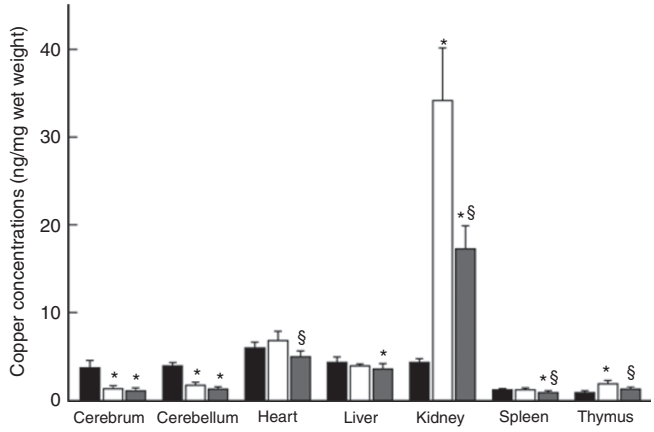

Figure 3. Copper concentrations in organs of control male mice and macular mice treated with cupric chloride ($CuCl_2$) or copper-pyruvaldehyde bis(N^4-methylthiosemicarbazone) (Cu-PTSM). Measured values in the control (black bar), $CuCl_2$-treated (white bar), and Cu-PTSM-treated mice (gray bar) are shown as means ± SD (in ng/mg wet weight, $n = 8$). *$P < 0.05$, $CuCl_2$-treated or Cu-PTSM-treated group vs. control group; §$P < 0.05$, $CuCl_2$-treated vs. Cu-PTSM-treated group.

in hematological data among $CuCl_2$- or Cu-PTSM-treated mice and their normal male siblings. There were no significant differences in biochemistry data for liver and renal function among the groups. Urinary β2-microglobulin, a biomarker for renal tubular function, did not rise in $CuCl_2$- or Cu-PTSM-treated mice.

DISCUSSION

The use of Cu-PTSM results in a relatively higher level of copper transport into the brain as bis(thiosemicarbazone) complexes (16,17). Cu-PTSM diffusively penetrates the cell membrane, and copper is liberated within cells through a reductive reaction (11). The principal source of Cu-PTSM reduction is NADH dehydrogenase in complex I of the mitochondrial

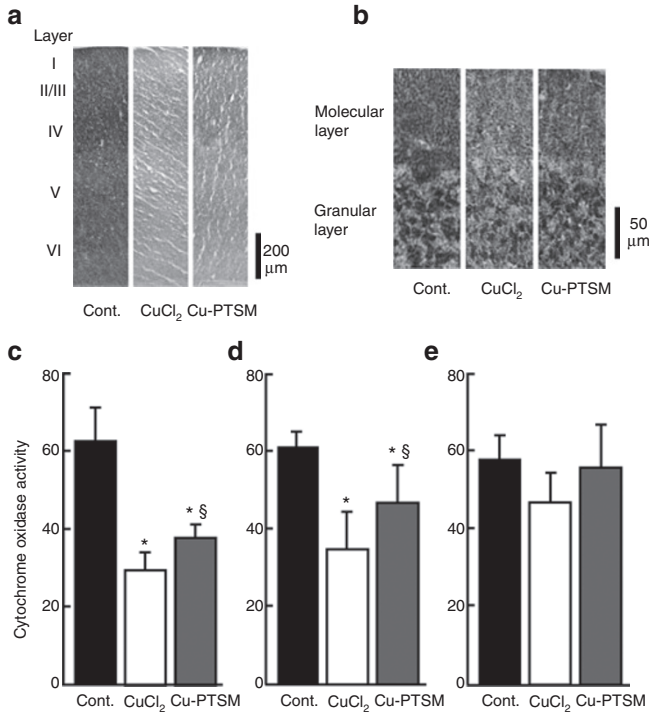

Figure 4. Results of cytochrome oxidase (CO) histochemistry in the cerebral (**a**) and cerebellar sections (**b**). In the cerebral cortex, layer IV of the somatosensory region was measured for CO activity (**c**). In the cerebellar hemispheric cortex, the molecular (**d**) and granular layers (**e**) were measured separately. Values are means ± SD ($n = 8$) in µmol/min/g of tissue. *$P < 0.05$, cupric chloride ($CuCl_2$)-treated or copper-pyruvaldehyde bis(N^4-methylthiosemicarbazone) (Cu-PTSM)-treated group vs. control; §$P < 0.05$, $CuCl_2$-treated vs. Cu-PTSM-treated group. Cont., control.

electron transport chain (18); reaction with intracellular sulfhydryl groups is an additional reduction mechanism (19). Copper carried by Cu-PTSM shows less selective distribution among various organelles, appearing in the nucleus, mitochondria, and microsomes, as well as in cytosol, thereby entering normal cellular pools for copper ions (10). In this study, macular mice, which would die within 2 wk after birth without treatment, survived with Cu-PTSM treatment, implying that copper carried by Cu-PTSM is used in systemic copper-dependent metabolism.

The copper distribution among organs in the Cu-PTSM-treated mice may be correlated with the homing pattern of Cu-PTSM (16,20). In a radiopharmaceutical study, 2–5% of the injected dose reached the brain, whereas large amounts of Cu-PTSM were transferred to the liver. In Cu-PTSM-treated mice, copper levels in the brain remained low, and copper in the liver was not much reduced. Therefore, a large amount of Cu-PTSM is likely to be trapped by the liver. Combined use of Cu-PTSM with a drug-delivery system to reduce liver trapping may increase copper delivery to the brain accordingly.

ATP7A expression in the brain becomes abundant in the early postnatal period, when neocortical neurons and endothelial cells show dense staining for ATP7A (21). In the brindled mouse, another MD model with impaired ATP7A function,

Table 2. Effects of $CuCl_2$ or Cu-PTSM treatment on hematological, biochemistry, and urinary data in macular mice

	Controls	$CuCl_2$	Cu-PTSM	*P* value
Hematological parameters				
WBC (10^3/mm^3)	2.1 ± 0.3	2.4 ± 1.6	2.6 ± 0.9	0.51
RBC (10^6/mm^3)	6.8 ± 0.8	7.0 ± 0.4	7.0 ± 0.5	0.96
Hb (g/dl)	11.2 ± 1.0	11.0 ± 1.1	10.5 ± 0.8	0.87
Hct (%)	39.0 ± 4.3	37.2 ± 1.9	37.5 ± 2.5	0.44
Plt (10^3/mm^3)	785 ± 94	760 ± 100	849 ± 88	0.33
Plasma biochemistry				
AST (IU/l)	51 ± 13	55 ± 5	55 ± 13	0.40
ALT (IU/l)	32 ± 15	39 ± 20	32 ± 9	0.64
BUN (mg/dl)	27.9 ± 4.0	28.1 ± 7.8	26.3 ± 3.2	0.63
Cr (mg/dl)	0.12 ± 0.02	0.10 ± 0.03	0.11 ± 0.02	0.19
Urine				
β2-M (μg/gCr)	96.1 ± 25.1	68.4 ± 27.3	75.7 ± 26.3	0.09

Data are shown as mean ± SD (n = 7–8). *P* values were determined using the Kruskal–Wallis test.

ALT, alanine aminotransferase; AST, aspartate aminotransferase; BUN, blood urea nitrogen; Cr, creatinine; $CuCl_2$, cupric chloride; Cu-PTSM, copper-pyruvaldehyde bis(N^4-methylthiosemicarbazone); Hb, hemoglobin concentration; Hct, hematocrit; Plt, platelets; RBC, red blood cell counts; WBC, white blood cell counts; β2-M, β2-microglobulin.

dense copper deposition is found in endothelial cells from early infancy (22). Therefore, ATP7A plays a pivotal role in the passage of copper across the blood–brain barrier, especially in the developing brain. In addition, copper delivery from glia to neurons is also mediated by ATP7A (23). Unusual copper deposits in these cells were counted in the gross copper levels of the brain in our study, but these deposits may not actually be used by neurons.

As CO requires copper for its activity, cerebral CO activity in MD is reduced and causes mitochondrial malfunction (24,25). With effective delivery of copper into the brain across the blood–brain barrier, cuproenzymes, including CO in neurons, would exhibit increased activity. As glia contribute minimally to overall CO activity, changes in optical density of CO histochemistry indicate the changes in neuronal CO activity (26). In our study, CO activity in the cerebral and cerebellar cortex in Cu-PTSM-treated mice was significantly higher than in $CuCl_2$-treated mice. This suggests that copper carried by Cu-PTSM was delivered more effectively to neurons, to activate CO, than copper carried by $CuCl_2$. Cu-PTSM can diffuse across cell membranes to reach neurons because of its high lipophilicity. In addition, the release of copper by NADH dehydrogenase is facilitated by high NADH levels (18,27). As the $NADH/NAD^+$ ratio in cells with CO malfunction is high (28), Cu-PTSM may effectively relieve copper deficits in the encephalic neurons of the macular mouse.

Cu-PTSM is a safe radiopharmaceutical for use in human clinical studies; a single shot of Cu-PTSM had no effect on hematological or biochemical values in humans (20). However, at higher doses, the toxicity of Cu-PTSM should be considered, such as might be the case with copper replacement therapy. PTSM without chelated Cu is not toxic (median lethal dose (p.o.) > 4 g/kg in mice) (29), whereas nonradiolabeled Cu-PTSM exerts acute toxicity with a median lethal dose (i.v.) of 26 mg/kg in rats and causes a transient increase in alanine aminotransferase value in surviving animals (30). The histopathological evaluation revealed that the lung was the primary target organ for Cu-PTSM, which may reflect Cu-mediated oxidative injury. Although Cu-PTSM at the dose used in this study seemed not to affect the functions of the major organs in the mice, the extent of toxic effects of Cu-PTSM is largely unknown in humans and requires further investigation.

Mild renal tubular dysfunction can occur in a subset of patients with MD; urinary β2-microglobulin, a low-molecular-weight protein absorbed at the proximal tubule, increases with age, whereas other biochemical indicators of renal function remain normal (31,32). Dysfunction is caused by significant copper accumulation in the renal tubule. In macular mice, copper accumulated at high levels in the renal tubules during 1 mo of treatment with $CuCl_2$ (6). In our study, copper accumulation in the Cu-PTSM-treated group was lower than that in the $CuCl_2$-treated group. By radiopharmacology, the renal uptake of Cu-PTSM is relatively low, with a trace level of urinary secretion, despite high blood flow to the kidneys; this may explain the relatively lower copper accumulation with Cu-PTSM. In this study, urinary β2-microglobulin secretion did not increase in either the $CuCl_2$-treated or Cu-PTSM-treated groups. However, in considering long-term copper supplementation for MD, the decrease in renal copper accumulation with Cu-PTSM may be beneficial in terms of copper-mediated oxidative injury.

In conclusion, although the copper-trafficking efficacy of Cu-PTSM was limited, Cu-PTSM effectively increased neuronal CO activity. The reduction in copper accumulation in the kidney would seem to be advantageous. These findings support further study of therapeutic potential of Cu-PTSM for MD.

METHODS

Drugs

Cu-PTSM was synthesized by Fuji Molecular Planning (Yokohama, Japan), as described by Green *et al.* (8), with the use of elemental copper instead of radioactive copper. Solvents applicable for Cu-PTSM are limited because of its strong lipophilicity. In this study, DMSO (Sigma, St Louis, MO) was used because of its excellent ability to dissolve Cu-PTSM (33). $CuCl_2$ (Wako, Tokyo, Japan) was dissolved in saline.

Animals

Normal C3H male mice, 15–17 d old, were used in acute toxicity studies for $CuCl_2$, Cu-PTSM, and DMSO. In a copper-supplement study in the MD model mice, male hemizygous macular mice and normal littermate controls were used. Macular mice arose from the $C3H_f$ inbred strain and possess a single base change (4223T→C, exon 22) in the *Atp7a* gene (14,15). All procedures involving animals were approved by the Animal Care and Use Committees of the Tohoku University School of Medicine and Teikyo University School of Medicine.

Acute Toxicity Studies

Saline (0.01 ml), DMSO (0.01 ml), $CuCl_2$ (25 μg in 0.01 ml saline), or Cu-PTSM (57 μg in 0.01 ml DMSO) was injected subcutaneously into 15–17-d-old normal male C3H mice. The doses of $CuCl_2$ or Cu-PTSM contain the same amount of copper, corresponding to that in subsequent experiments in macular mice. Then, 24 h later, the mice were anesthetized with ether, and blood was sampled. The hematological parameters were determined using a veterinary hematology analyzer (LC-152; Horiba, Kyoto, Japan). Blood chemistry parameters were measured using a biochemistry analyzer (Hitachi 7180; Hitachi, Tokyo, Japan).

Copper Supplement in Macular Mice

Macular mice were treated with subcutaneous injections of $CuCl_2$ or Cu-PTSM solution postnatally on days 4, 10, and 17 with a microsyringe. The doses of $CuCl_2$ and Cu-PTSM on the first injection day (day 4) were 20 and 46 μg, respectively, whereas those on the second and third injection days (days 10 and 17) were 25 and 57 μg, respectively. The doses of Cu-PTSM contained the same amount of copper as in the $CuCl_2$ given in each injection.

At 4 wk of age, control and surviving $CuCl_2$- and Cu-PTSM-treated mice were deeply anesthetized with ether and decapitated. The organs were weighed, and samples of organ tissues (~50 mg) were kept in an acid-washed perfluoroalkoxy vessel to measure tissue copper levels. Simultaneously, the unfixed cerebrum and cerebellum were quickly embedded in optimal cutting temperature compound (Sakura Finetechnical, Tokyo, Japan) and frozen on dry ice for cytochrome oxidase histochemistry. All samples were then kept at −80 °C until analysis.

In separate experiments, urine was collected from another set of $CuCl_2$- and Cu-PTSM-treated mice, as well as from their male siblings, at 4 wk of age. Mice were then anesthetized, and blood was sampled. Urinary β2-microglobulin was measured by enzyme-linked immunosorbent assay (USCN Life Science, Wuhan, China), and samples were used for hematological and biochemistry analysis as described above.

Tissue Copper Levels

Tissue copper levels were measured as described in previous reports, using an inductively coupled plasma-mass spectrometer (ELAN DRC-e; PerkinElmer SCIEX, Concord, ON, Canada) (34). Briefly, the tissue samples were digested with 2 ml of high-purity HNO_3 (Wako) at 120 °C for 2 h and dried. The processed samples were dissolved completely with 2% HNO_3 to a final volume of 10 ml. Indium (^{115}In) solution was routinely added to the samples as an internal standard to normalize analyte signal intensities for quantitative analysis. Then, the copper (^{65}Cu) concentration was measured with an inductively coupled plasma-mass spectrometer.

CO Histochemistry in the Brain

Duplicate series of sections from each brain were prepared for CO histochemistry using the protocol described previously (35,36), with several modifications. Briefly, the frontal lobes of the brains were coronally sectioned (20 μm thick) in a cryostat microtome at −20 °C and mounted on silanized slides. A set of CO activity standards was also sectioned (20 μm thick) and mounted on each slide. The slides were then kept refrigerated at −80 °C until staining with diaminobenzidine. The sections were incubated at 37 °C for 2 h in the dark in a staining medium containing 120 ml of 0.1 mol/l phosphate buffer (pH 7.4), 60 mg of 3,3′-diaminobenzidine (Sigma), 18 mg of cytochrome c (Sigma), 3 mg of catalase (Sigma), and 4.8 g of sucrose (Wako). The sections were then dehydrated in ethanol, cleared in xylene, and coverslipped.

Photographs of the brain and standard block slices stained for CO histochemistry were obtained in 8-bit grayscale mode with a microscope (BX-61; Olympus, Tokyo, Japan) equipped with a digital camera (DP-70; Olympus). Regions of interest in stained slices were determined using a mouse brain atlas (37). Layer IV of the cerebral cortex somatosensory region and the molecular and granular layers of the hemispheric cortices of the cerebellum were measured. Grayscale values of these regions of interest were measured by densitometry using a custom-made program developed with LabVIEW (National Instruments, Austin, TX) and an image processing extension (VISION; National Instruments); the pixel values in the regions of interest and control were averaged and transformed to CO activity using a Kodak grayscale tablet with known optical density values. Cracks in a slice were programmatically removed from the analysis. The strong correlation between staining density and regional CO activity has been validated previously by Darriet *et al.* (38) and Gonzalez-Lima and Jones (39).

Preparation of CO Activity Standards

Standards with known CO activity were developed to quantitatively determine enzyme activity in the histochemical material. Six 4-wk-old rats were deeply anaesthetized with ether and perfused with cooled 0.1 mol/l phosphate buffer, and the brains were extracted and homogenized in ice. Half of the homogenized brain paste was heated in an incubator at 60 °C for 5 h to inactivate CO activity, whereas the other half was kept at −20 °C. Three mixtures of active and inactive pastes were made with three different mixture ratios. Each paste was frozen in a silicon tube (3 mm internal diameter) at −80 °C to make cylindrical blocks of paste (3 mm outer diameter × 10 mm length). These blocks were embedded together in optimal cutting temperature

compound and kept at −80 °C. A small amount (~6 mg) of each mixed paste was separately pretreated in cooled *n*-dodecyl β-D-maltoside buffer for 15 min, and CO activity was measured using a spectrophotometric method (cytochrome c oxidase activity assay kit; BioChain, Hayward, CA) at room temperature (25 °C).

Statistical Analyses

Data are shown as the means ± SD. Statistical analyses of data, except data for CO activity, were performed by the Kruskal–Wallis test followed by the Steel–Dwass test for multiple comparisons among the groups. CO activity measurements were analyzed by one-way factorial ANOVA after confirming a normal distribution of data, followed by a *post hoc* Fisher's protected least significant difference test. For all tests, values of $P < 0.05$ were considered to indicate statistical significance.

ACKNOWLEDGMENTS

We thank Yoshimasa Sakamoto, Makoto Miyagawa, Wataru Takimoto, Aoi Takemata, Yoko Chiba, Shinichiro Shimada, Mio Miyazawa, and Yayoi Takahashi for providing technical assistance.

STATEMENT OF FINANCIAL SUPPORT

This research was supported by a Grant-in-Aid for Exploratory Research to Mitsutoshi Munakata from the Ministry of Education, Culture, Sports, Science and Technology of Japan. The authors declared no conflict of interest.

REFERENCES

1. Kodama H, Murata Y. Molecular genetics and pathophysiology of Menkes disease. Pediatr Int 1999;41:430–5.
2. Lutsenko S, Barnes NL, Bartee MY, Dmitriev OY. Function and regulation of human copper-transporting ATPases. Physiol Rev 2007;87:1011–46.
3. Kodama H, Fujisawa C. Copper metabolism and inherited copper transport disorders: molecular mechanisms, screening and treatment. Metallomics 2009;1:42–52.
4. Sherwood G, Sarkar B, Kortsak AS. Copper histidinate therapy in Menkes' disease: prevention of progressive neurodegeneration. J Inherit Metab Dis 1989;12:Suppl 2:393–6.
5. Sarkar B, Lingertat-Walsh K, Clarke JT. Copper-histidine therapy for Menkes disease. J Pediatr 1993;123:828–30.
6. Kodama H, Sato E, Gu YH, Shiga K, Fujisawa C, Kozuma T. Effect of copper and diethyldithiocarbamate combination therapy on the macular mouse, an animal model of Menkes disease. J Inherit Metab Dis 2005;28:971–8.
7. Tanaka K, Kobayashi K, Fujita Y, Fukuhara C, Onosaka S, Min K. Effects of chelators on copper therapy of macular mouse, a model animal of Menkes' kinky disease. Res Commun Chem Pathol Pharmacol 1990;69:217–27.
8. Green MA, Klippenstein DL, Tennison JR. Copper(II) bis(thiosemicarbazone) complexes as potential tracers for evaluation of cerebral and myocardial blood flow with PET. J Nucl Med 1988;29:1549–57.
9. Green MA, Mathias CJ, Welch MJ,et al. Copper-62-labeled pyruvaldehyde bis(N4-methylthiosemicarbazonato)copper(II): synthesis and evaluation as a positron emission tomography tracer for cerebral and myocardial perfusion. J Nucl Med 1990;31:1989–96.
10. Baerga ID, Maickel RP, Green MA. Subcellular distribution of tissue radiocopper following intravenous administration of ^{67}Cu-labeled Cu-PTSM. Int J Rad Appl Instrum B 1992;19:697–701.
11. Fujibayashi Y, Wada K, Taniuchi H, Yonekura Y, Konishi J, Yokoyama A. Mitochondria-selective reduction of ^{62}Cu-pyruvaldehyde bis(N4-methylthiosemicarbazone) (^{62}Cu-PTSM) in the murine brain; a novel radiopharmaceutical for brain positron emission tomography (PET) imaging. Biol Pharm Bull 1993;16:146–9.
12. Mercer JF. Menkes syndrome and animal models. Am J Clin Nutr 1998;67(5 Suppl):1022S–8S.
13. Yamano T, Shimada M, Kawasaki H, Onaga A, Nishimura M. Clinico-pathological study on macular mutant mouse. Acta Neuropathol 1987;72:256–60.
14. Mori M, Nishimura M. A serine-to-proline mutation in the copper-transporting P-type ATPase gene of the macular mouse. Mamm Genome 1997;8:407–10.
15. Murata Y, Kodama H, Abe T,et al. Mutation analysis and expression of the mottled gene in the macular mouse model of Menkes disease. Pediatr Res 1997;42:436–42.
16. Blower PJ, Lewis JS, Zweit J. Copper radionuclides and radiopharmaceuticals in nuclear medicine. Nucl Med Biol 1996;23:957–80.
17. Dearling JL, Lewis JS, Mullen GE, Rae MT, Zweit J, Blower PJ. Design of hypoxia-targeting radiopharmaceuticals: selective uptake of copper-64 complexes in hypoxic cells *in vitro*. Eur J Nucl Med 1998;25:788–92.
18. Taniuchi H, Fujibayashi Y, Okazawa H, Yonekura Y, Konishi J, Yokoyama A. Cu-pyruvaldehyde-bis(N^4-methylthiosemicarbazone) (Cu-PTSM), a metal complex with selective NADH-dependent reduction by complex I in brain mitochondria: a potential radiopharmaceutical for mitochondria-functional imaging with positron emission tomography (PET). Biol Pharm Bull 1995;18:1126–9.
19. Minkel DT, Saryan LA, Petering DH. Structure–function correlations in the reaction of bis(thiosemicarbazonato) copper(II) complexes with Ehrlich ascites tumor cells. Cancer Res 1978;38:124–9.
20. Wallhaus TR, Lacy J, Whang J, Green MA, Nickles RJ, Stone CK. Human biodistribution and dosimetry of the PET perfusion agent copper-62-PTSM. J Nucl Med 1998;39:1958–64.
21. Niciu MJ, Ma XM, El Meskini R, Ronnett GV, Mains RE, Eipper BA. Developmental changes in the expression of ATP7A during a critical period in postnatal neurodevelopment. Neuroscience 2006;139:947–64.
22. Yoshimura N. Histochemical localization of copper in various organs of brindled mice. Pathol Int 1994;44:14–9.
23. Kodama H, Meguro Y, Abe T,et al. Genetic expression of Menkes disease in cultured astrocytes of the macular mouse. J Inherit Metab Dis 1991;14:896–901.
24. Maehara M, Ogasawara N, Mizutani N, Watanabe K, Suzuki S. Cytochrome c oxidase deficiency in Menkes kinky hair disease. Brain Dev 1983;5:533–40.
25. Munakata M, Sakamoto O, Kitamura T,et al. The effects of copper-histidine therapy on brain metabolism in a patient with Menkes disease: a proton magnetic resonance spectroscopic study. Brain Dev 2005;27:297–300.
26. Wong-Riley MT. Cytochrome oxidase: an endogenous metabolic marker for neuronal activity. Trends Neurosci 1989;12:94–101.
27. Taniuchi H, Fujibayashi Y, Yonekura Y, Konishi J, Yokoyama A. Hyperfixation of copper-62-PTSM in rat brain after transient global ischemia. J Nucl Med 1997;38:1130–4.
28. Wijburg FA, Feller N, Scholte HR, Przyrembel H, Wanders RJ. Studies on the formation of lactate and pyruvate from glucose in cultured skin fibroblasts: implications for detection of respiratory chain defects. Biochem Int 1989;19:563–70.
29. Petering HG, Buskirk HH, Underwood GE. The anti-tumor activity of 2-keto-3-ethoxybutyraldehyde bis(thiosemicarbazone) and related compounds. Cancer Res 1964;24:367–72.
30. Kostyniak PJ, Nakeeb SM, Schopp EM,et al. Acute toxicity and mutagenicity of the copper complex of pyruvaldehyde-bis (N-4-methylthiosemicarbazone), Cu-PTSM. J Appl Toxicol 1990;10:417–21.
31. Ozawa H, Kodama H, Kawaguchi H, Mochizuki T, Kobayashi M, Igarashi T. Renal function in patients with Menkes disease. Eur J Pediatr 2003;162:51–2.
32. Kodama H, Okabe I, Kihara A, Mori Y, Okaniwa M. Renal tubular function of patients with classical Menkes disease. J Inherit Metab Dis 1992;15:157–8.
33. David NA. The pharmacology of dimethyl sulfoxide. Annu Rev Pharmacol 1972;12:353–74.
34. Thomas R. Practical Guide to ICP-MS. New York, NY: Marcel Dekker, 2004; pp. 207–44.

35. Wong-Riley M. Changes in the visual system of monocularly sutured or enucleated cats demonstrable with cytochrome oxidase histochemistry. Brain Res 1979;171:11–28.
36. Strazielle C, Krémarik P, Ghersi-Egea JF, Lalonde R. Regional brain variations of cytochrome oxidase activity and motor coordination in Lurcher mutant mice. Exp Brain Res 1998;121:35–45.
37. Franklin KB, Paxinos G. The mouse brain in stereotaxic coordinates. San Diego, California: Academic Press, 1944.
38. Darriet D, Der T, Collins RC. Distribution of cytochrome oxidase in rat brain: studies with diaminobenzidine histochemistry *in vitro* and [14C]cyanide tissue labeling *in vivo*. J Cereb Blood Flow Metab 1986;6:8–14.
39. Gonzalez-Lima F, Jones D. Quantitative mapping of cytochrome oxidase activity in the central auditory system of the gerbil: a study with calibrated activity standards and metal-intensified histochemistry. Brain Res 1994;660:34–49.